DTU Library

Backlash Estimation for Industrial Drive-Train Systems

Papageorgiou, Dimitrios; Blanke, Mogens; Niemann, Hans Henrik; Richter, Jan H.

Published in:
Preprints of the 20th World Congress

Link to article, DOI:
10.1016/j.ifacol.2017.08.621

Publication date:
2017

Document Version
Peer reviewed version

Preprints of the 20th World Congress
The International Federation of Automatic Control
Toulouse, France, July 9-14, 2017

Backlash estimation for industrial drive-train systems

Dimitrios Papageorgiou * **Mogens Blanke** *,** **Hans Henrik Niemann** *
Jan H. Richter ***

* *Department of Electrical Engineering, Automation and Control, Technical University of Denmark, DK-2800 Kgs. Lyngby, Denmark, (e-mail: dimpa,mb,hhn@elektro.dtu.dk).*
** *AMOS CoE, Institute of Technical Cybernetics, Norwegian University of Science and Technology, Trondheim, Norway*
*** *Siemens AG, Digital Factory Division, D-90475 Nuremberg, Germany, (e-mail: janrichter@siemens.com)*

Abstract: Backlash in gearing and other transmission components is a common positioning-degrading phenomenon that develops over time in industrial machines. High-performance machine tool controls use backlash compensation algorithms to maintain accurate positioning of the tool to cope with such deadzone phenomena. As such, estimation of the magnitude of deadzones is essential. This paper addresses the generic problem of accurately estimating the width of the deadzone in a single-axis mechanical drive train. The paper suggests a scheme to estimate backlash between motor and load, employing a sliding mode observer and a nonlinear adaptive estimator. The efficacy of the approach is illustrated via simulations.

Keywords: adaptive deadzone estimation, mechanical drive-train, parameter estimation, sliding-mode observer, nonlinear parametrization

1. INTRODUCTION

Developing backlash due to wear in spindles, gears, clutches and guides is one of the main reasons for performance degradation in machine tool systems. Since high precision tool positioning is fundamental for obtaining the required quality of the machined end-products, backlash compensation is used in nearly all modern Computer Numerical Control (CNC) algorithms. Compensation necessitates knowledge of the backlash offset angle so that it can be used in the position servo loops that control motors on the machine's axes. In such context, online estimation methods may facilitate automatic compensation for developing backlash.

A substantial amount of research has been conducted on estimation of the backlash phenomenon for various systems over the past three decades. In Stein and Wang [1998] the backlash in a gearing system was indirectly estimated by calculating the bounce, i.e. the change of the speed of the driving part of the gear due to the backlash impact when exiting the deadzone. Extended Kalman Filter (EKF) was employed in Hovland et al. [2002] for estimating a backlash torque in a two-mass motor arm, based on torque and position measurements. Modelling of backlash torque was presented in Merzouki and Cadiou [2005], who used a differentiable function to represent backlash and suggested a nonlinear observer for estimation of backlash amplitude. This method was validated experimentally in Merzouki et al. [2007], in which a sliding mode observer was used for estimation of backlash torque. Based on this estimation, backlash function parameters were identified offline. The effect of the deadband due to backlash in a closed loop motion system was studied in Hågglund [2007] using describing functions. The function parameters were calculated online using a static relation for controller gains. Backlash in automotive powertrains was described in Lagerberg and Egardt [2003] based on position difference between drive motor and load. A Kalman filter was shown to estimate backlash within 10% error. A four-parameter model was used in Vörös [2010] to describe backlash effects in generic linear cascaded systems. The backlash identification was treated as a quasi-linear problem such that iterative algorithms could be used. Minimization of a quadratic prediction error was employed in Templin [2008], where position, velocity and torque measurements were used for offline identification of backlash torques in a vehicle drive-line system.

In the previous approaches, the backlash phenomenon was described through the resulting torque upon contact of two parts of a coupling. In the cases where the deadzone angle was identified directly, this was done offline or around a linearization point of the system. The previous results showed the need for new ideas for high accuracy estimation of backlash if compensation shall be useful in machinery systems where very high precision is required.

This paper considers the problem of designing a dynamic estimator for the deadzone angle of a developing backlash in a single-axis drive-train system. The proposed method employs modelling of backlash in terms of variable shaft stiffness, depending on the deadzone size, and it addresses the requirement for fast and accurate estimation of the deadzone angle. Similarly to Merzouki et al. [2007], a second order Super-twisting Sliding Mode observer (STSMO) is used to estimate the backlash torque. This value is utilized by an adaptive estimator designed with the purpose to determine the deadzone angle.

The paper is organized as follows: Section 2 states the problem in concise terms, describing the drive-train system as an ab-

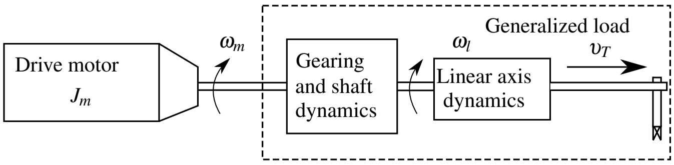

Fig. 1. Correspondence between mechanical drive-train and single-axis machine-tool systems. The angular velocities of the motor and the load are denoted by ω_m, ω_l, respectively, while υ_T is the tool linear velocity.

straction of a single-axis machine tool, and presents a model for backlash based on varying shaft stiffness. The design of the parameter estimator is presented in Section 3 and Section 4 presents results obtained from high fidelity simulations. Finally, conclusions are drawn and results are discussed in Section 5.

2. SYSTEM DESCRIPTION AND PROBLEM FORMULATION

A typical single-axis machine tool consists of a linear axis, which positions the tool. The axis is actuated by a drive motor that is typically connected to an angular-to-linear motion conversion device (e.g. a ball-screw).

The combined elasticity, friction, damping and total mass of all the mechanical components that connect to the drive shaft can be lumped into a generalised load. The single-axis machine tool can then be viewed as a mechanical drive train comprising the drive motor, a flexible shaft with damping and backlash, and a load with friction as show in Figure 1.

2.1 Drive train modelling

With identification of backlash being in focus of this work, angular accelerations, velocities and difference of angles between mechanical components are essential. Torque produced by the drive motor is measured, hence the closed-loop electrical dynamics of the motor need not be considered. An overview of the most important variables and notation used in the modelling of the system is provided in Table 1.

The dynamics of the mechanical drive-train system reads:

Table 1. System model nomenclature

Symbol	Description	Units
States and Outputs		
ω_m, ω_l	Motor/load angular velocity	$\mathrm{rad\,s^{-1}}$
θ_m, θ_l	Motor/load angular position	rad
Inputs and disturbances		
u	Torque command	$\mathrm{N\,m}$
$T_{F,m}, T_{F,l}$	Motor/load friction	$\mathrm{N\,m}$
T_l	Interconnection/backlash torque	$\mathrm{N\,m}$
Constant parameters		
J_m, J_l	Motor/load inertia	$\mathrm{kg\,m^2}$
K_S	Shaft stiffness	$\mathrm{N\,m\,rad^{-1}}$
D_S	Shaft damping coefficient	$\mathrm{N\,m\,s\,rad^{-1}}$
N	Gearing ratio	–
$T_{C,m}, T_{C,l}$	Coulomb friction on the motor/load	$\mathrm{N\,m}$
β_m, β_l	Motor/load viscous friction coefficient	$\mathrm{N\,m\,s\,rad^{-1}}$
δ	Deadzone angle	rad

$$\dot{\omega}_m = \frac{1}{J_m}u - \frac{1}{J_m}T_{F,m} - \frac{1}{NJ_m}T_l \tag{1}$$
$$\dot{\theta}_m = \omega_m \tag{2}$$
$$\dot{\omega}_l = -\frac{1}{J_l}T_{F,l} + \frac{1}{J_l}T_l \tag{3}$$
$$\dot{\theta}_l = \omega_l \ . \tag{4}$$

In the backlash-free case the interconnecting torque T_l is given from:

$$T_l = K_S\left(\frac{1}{N}\theta_m - \theta_l\right) + D_S\left(\frac{1}{N}\omega_m - \omega_l\right) \tag{5}$$

where K_S, D_S and N are defined in Table 1 and are assumed to be known. The friction torques acting on the drive motor and the load are modelled as described in the following equation (Egeland and Gravdahl [2002]):

$$T_{F,i} = T_{C,i}\mathrm{sgn}(\omega_i) + \beta_i\omega_i, \ i \in \{m, l\} \tag{6}$$

where $\mathrm{sgn} : \mathbb{R} \to \{-1, 0, 1\}$ is the signum function defined as:

$$\mathrm{sgn}(\xi) = \begin{cases} 1 & \text{if } \xi > 0 \\ 0 & \text{if } \xi = 0 \\ -1 & \text{if } \xi < 0 \ . \end{cases} \tag{7}$$

and the parameters $\beta_m, \beta_l, T_{C,m}, T_{C,l}$ are considered known and constant.

2.2 Backlash modelling

Backlash is the effect of sudden disengagement between drive motor and load as shown in Figure 2. A number of static and dynamic models have been developed, based on the interconnecting (restoring and damping) torque in a mass-spring-damper system (see for example Nordin et al. [1997]; Gerdes and Kumar [1995]; de Marchi [1998] and Nordin and Gutman [2002]). The most intuitive and common one is the deadzone model presented by Nordin et al. [1997], in which the interconnecting torque T_l becomes zero inside the deadzone, while outside of it the angle difference (between motor and load) is offset by the width of the deadzone angle.

Although the existing backlash models can accurately describe the phenomenon, the discontinuities that they contain make these models difficult to use in control and estimation design. A model for backlash, which is based on changing shaft stiffness, will be presented in this section and compared to the deadzone model. This model will subsequently be used for deadzone estimation and monitoring.

Defining the angular position and velocity differences between drive motor and load as

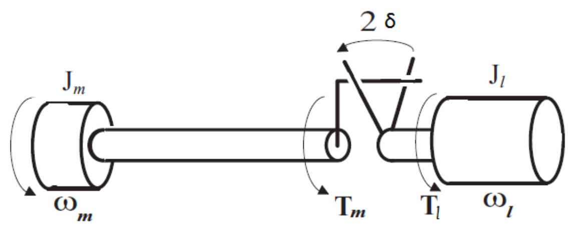

Fig. 2. Backlash: When the difference between the motor and the load position is smaller than δ, then the two shafts are disengaged and no torque is applied to the motor or the load. The picture is taken from Nordin and Gutman [2002].

$$\Delta\theta \triangleq \frac{1}{N}\theta_m - \theta_l \tag{8}$$

$$\Delta\omega \triangleq \frac{1}{N}\omega_m - \omega_l \tag{9}$$

the interconnection torque T_l in the deadzone model is given by

$$T_l^{DZ} = \begin{cases} K_S(\Delta\theta - \delta\cdot\mathrm{sgn}(\Delta\theta)) + D_S\Delta\omega & , |\Delta\theta| > \delta \\ 0 & , |\Delta\theta| \leq \delta\ . \end{cases} \tag{10}$$

The proposed model is based on factorization of the backlash torque as a function of shaft stiffness. The latter is very small, virtually zero, when inside the deadzone, and assumes its nominal value outside of it. The transition between the two extreme values of the stiffness is fast but smooth. The corresponding torque reads:

$$T_l = \left[\Delta\theta - \delta\cdot\mathrm{sgn}(\Delta\theta) + \frac{D_S}{K_S}\Delta\omega\right]\cdot K_{BL}(\Delta\theta,\delta) \tag{11}$$

$$K_{BL} = \frac{K_S}{\pi}\left[\pi + \arctan(\alpha(\Delta\theta-\delta)) - \arctan(\alpha(\Delta\theta+\delta))\right] \tag{12}$$

The positive constant α expresses the rate of change in the stiffness as it can be seen in Figure 3. For $\alpha\to\infty$, it is clear that $T_l \to T_l^{DZ}$.

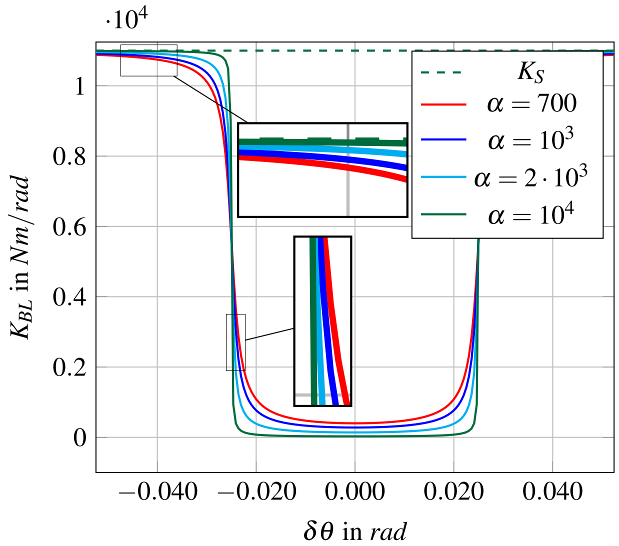

Fig. 3. Shaft stiffness varying between two values. The larger the value of α, the steeper the change in the stiffness is.

2.3 Problem formulation

The collective objective can be summarised in the following problem formulation:

Problem 1. (Deadzone angle estimation). Given the single-axis drive-train system described in (1)-(6) and the backlash model in (11),(12), design an online dynamic estimator for the deadzone angle δ with the following requirements:

- Maximum steady-state estimation error less than 10^{-3} rad.
- Asymptotic convergence to the real parameter value.

3. BACKLASH DEADZONE ANGLE ESTIMATION

Estimation of the deazone angle belongs to a family of problems of online parameter estimation in systems with nonlinear parametrization that has been treated in numerous works in the literature. The approach followed in this paper is based on a method for parameter estimation in nonlinearly parametrized systems presented in Grip et al. [2010]. The basic idea relates to estimating a perturbation of the system dynamics that depends on the unknown parameter and then finding an adaptive law for estimating the parameter itself.

3.1 Method overview

Consider that the system dynamics is described by

$$\dot{x} = f(x) + g(x)\left[u(x) + d(x,\delta)\right] \tag{13}$$

where $x\in\mathbb{R}^n$ is measured, $f:\mathbb{R}_{\geq 0}\times\mathbb{R}^n\to\mathbb{R}^n$ and $g:\mathbb{R}_{\geq 0}\times\mathbb{R}^n\to\mathbb{R}^{n\times m}$ are the unforced system dynamics and gain, respectively, which can be evaluated from the measurements, $\delta\in\mathscr{D}\subset\mathbb{R}$ is the unknown parameter, $u\in\mathbb{R}^m$ is the control input and $d:\mathbb{R}_{\geq 0}\times\mathbb{R}^n\times\mathscr{D}\to\mathbb{R}^m$ is a matched disturbance vector, which can be evaluated if δ is known. The method pertains to finding an estimation $\hat{\phi}$ of the perturbation

$$\phi \triangleq g(x)d(x,\delta) \tag{14}$$

and then derive an adaptive law

$$\dot{\hat{\delta}} = \rho(x,\hat{\phi},\hat{\delta}) \tag{15}$$

for estimating the unknown parameter.

Regarding the drive-train system, all states are measured and the unknown parameter δ affects the dynamics of both the motor and the load in the same way, i.e. through the torque T_l. We can then choose either of the subsystems in (1), (3) on which to apply the method. For simplicity, the load velocity dynamics is chosen. The system can be written in the form of (13) with

$$f(x) \equiv f(\omega_l) = \frac{1}{J_l}T_{F,l}$$

$$g(x) \equiv g = \frac{1}{J_l}$$

$$d(x,\delta) = T_l\ ,$$

where T_l has been defined in (11), (12) and

$$x \triangleq [\omega_m\ \ \theta_m\ \ \omega_l\ \ \theta_l]^T$$

is the state vector of the drive-train system. The method is divided in two parts: estimation of the perturbation ϕ and derivation of the adaptive law $\rho(x,\hat{\phi},\hat{\delta})$.

3.2 Sliding mode perturbation observer

A second-order Sliding Mode Observer (SMO) was used for finding an estimate of ϕ. In general SMOs can offer finite-time estimation of unmeasured states by using high-frequency injection signals in their design, which depend on the observer innovation term (i.e. the error between real and predicted output) as shown in Shtessel et al. [2014]. By doing so, the estimation error dynamics reaches the *sliding manifold*, i.e. a manifold on which the error and its first time derivative are zero, and remain so thereafter. This provides at the same time an estimation of any unknown perturbations that affects the system dynamics (Fridman et al. [2011]). This idea can be clarified as follows.

Consider the load velocity dynamics presented in (3) and a SMO given by

$$\dot{\hat{\omega}}_l = -\frac{1}{J_l}T_{F,l} + v(\tilde{\omega}_l) \tag{16}$$

where $\tilde{\omega}_l = \omega_l - \hat{\omega}_l$ is the state estimation error and v is an appropriate high frequency term depending on the error signal

$\tilde{\omega}_l$. Define the sliding manifold $S = \{\tilde{\omega}_l \in \mathbb{R} : \tilde{\omega}_l = \dot{\tilde{\omega}}_l = 0\}$. The dynamics of the state estimation error reads:

$$\dot{\tilde{\omega}}_l = \dot{\omega}_l - \dot{\hat{\omega}}_l = \frac{1}{J_l} T_l - v \,. \tag{17}$$

If the error dynamics reaches the sliding manifold, then $\dot{\tilde{\omega}}_l = \tilde{\omega}_l = 0$ for all future times, which means that $v = \frac{1}{J_l} T_l$. In other words, if the injection signal v is designed such that the estimation error dynamics reaches the sliding manifold S and remains on the manifold thereafter, then the unknown perturbation $\phi = \frac{1}{J_l} T_l$ is estimated indirectly by v. The design of v can be obtained as in Levant [1993]:

$$v = k_1 |\tilde{\omega}_l|^{\frac{1}{2}} \mathrm{sgn}(\tilde{\omega}_l) + k_2 \int_0^t \mathrm{sgn}(\tilde{\omega}_l(\tau)) d\tau \tag{18}$$

where k_1, k_2 are positive gains. The resulting observer is referred to as the STSMO and it is proven in Davila et al. [2005] that for appropriate gains k_1, k_2, the term v brings the observer error dynamics onto the sliding manifold S. Hence, the unknown perturbation can be estimated by (18), where

$$\hat{\phi} = k_2 \int_0^t \mathrm{sgn}(\tilde{\omega}_l(\tau)) d\tau \,. \tag{19}$$

The choice of a second order SMO for a system of relative degree 1 (the subsystem is scalar) was made due to the property of higher order SMOs to alleviate the chattering in the injection and estimation signals (Shtessel et al. [2014]).

Remark 1. Finite-time estimation of ϕ is ensured by selecting v as in (18) with k_1, k_2 being appropriately chosen positive gains. One additional requirement is that $T_l, \dot{T}_l$ need be bounded, which is ensured by the boundedness of the state vector and the smoothness of the backlash model. However, the bound on $\dot{T}_l$ is proportional to α. This means that the closer the model is to the deadzone model, the larger this bound will be, which in turn leads to higher gains for the observer.

3.3 Adaptive backlash angle estimator

The estimator design is inspired by the method proposed in Grip et al. [2010] for the estimation of unknown parameters. For the rest of the analysis we consider that the unknown parameter δ lies in a compact set $\mathscr{D} \subset \mathbb{R}$, with $\dot{\delta} = 0$ and we define the backlash angle estimation error as $\tilde{\delta} = \delta - \hat{\delta}$.

Considering the dynamics of the load velocity expressed in the form of (13) with $g = \frac{1}{J_l}$ and $d(x, \delta) = T_l(x, \delta)$ defined in (10),(12), the adaptive estimator for the deadzone angle is given by (Grip et al. [2010]):

$$\dot{\hat{\delta}} = \rho(x, \hat{\phi}, \hat{\delta}) = \mathrm{Proj}\left[\hat{\delta}, \gamma\mu(x, \hat{\delta})\left(\hat{\phi} - \frac{1}{J_l} T_l(x, \hat{\delta})\right)\right] \tag{20}$$

with $\gamma > 0$ being the adaptive gain, $\hat{\phi}$ an asymptotic estimate of $\frac{1}{J_l} T_l$ and $\mathrm{Proj}(\cdot,\cdot)$ the projection operator defined in Appendix A. In the adaptive law (20) $\mu(x, \hat{\delta})$ is a real-valued function defined on $\mathbb{R}^4 \times \mathscr{D}$, bounded for bounded x, with the following property:

Property 1. For all pairs $\delta_1, \delta_2 \in \mathscr{D}$ and $\forall x \in \mathbb{R}$,

$$\mu(x, \delta_1) \frac{1}{J_l} \frac{\partial T_l}{\partial \delta}(x, \delta_2) \geq \sigma(x) \tag{21}$$

where $\sigma(x)$ is a non-negative real-valued function defined on $\mathbb{R}^4$ with the following two properties:

Property 2. There exists a positive real constant number $L > 0$ such that $\forall \delta_1, \delta_2 \in \mathscr{D}$,

$$\frac{1}{J_l} |T_l(x, \delta) - T_l(x, \hat{\delta})| \leq L\sqrt{\sigma(x)} |\tilde{\delta}| \,. \tag{22}$$

Property 3. There exist positive real numbers T, ε such that $\forall t \in \mathbb{R}_{\geq 0}$,

$$\int_t^{t+T} \sigma(x(\tau)) d\tau \geq \varepsilon \,. \tag{23}$$

Following a similar reasoning as the one in the proof of Proposition 4 in Grip et al. [2010], it can be shown that the estimation error $\tilde{\delta}$ converges asymptotically to 0, and uniformly in x if an asymptotic estimate of ϕ is available.

The design of the adaptive deadzone angle estimator includes steps to find suitable functions μ and σ with the properties (1)-(3). Selecting $\mu(x, \hat{\delta})$ as

$$\mu(x, \hat{\delta}) = \frac{1}{K_S^2} \frac{\partial T_l}{\partial \delta}(x, \hat{\delta}) \tag{24}$$

condition (21) is satisfied with

$$\sigma(x) = \frac{1}{K_S^2} \left(\frac{\partial T_l}{\partial \delta}\right)^2 = \frac{1}{\pi^2} \left[\chi_1(x, \hat{\delta}) + \chi_2(x, \hat{\delta})\right]^2 \tag{25}$$

where χ_1, χ_2 are defined as

$$\chi_1(x, \hat{\delta}) = \mathrm{sgn}(\Delta\theta) \cdot \left[\pi + \arctan(\alpha(\Delta\theta - \hat{\delta})) - \arctan(\alpha(\Delta\theta + \hat{\delta}))\right] \tag{26}$$

$$\chi_2(x, \hat{\delta}) = \left[\Delta\theta - \hat{\delta} \cdot \mathrm{sgn}(\Delta\theta) + \frac{D_S}{K_S} \Delta\omega\right] \cdot \left\{\frac{\alpha}{1 + \left[\alpha(\Delta\theta - \hat{\delta})\right]^2} + \frac{\alpha}{1 + \left[\alpha(\Delta\theta + \hat{\delta})\right]^2}\right\} \,. \tag{27}$$

Since x and $\sigma(x)$ are bounded and $\mathscr{D}$ is compact, it is easy to show that there exits $L > 0$, such that condition (22) holds. The inequality $\int_t^{t+T} \sigma(x(\tau)) d\tau \geq \varepsilon$ expresses a type of Persistence of Excitation (PE) condition. From (25)-(27) it can be seen that this condition does not hold if, during the time interval $[t, t+T]$, the system is always within the deadzone. This, however, is expected, since in that case, there is no engagement between motor and load, hence no information about the stiffness of the shaft that connects them.

The adaptive law for the parameter estimate $\hat{\delta}$ is finally given by:

$$\dot{\hat{\delta}} = \mathrm{Proj}\left\{\hat{\delta}, \gamma \frac{1}{K_S^2} \frac{\partial T_l}{\partial \delta}(x, \hat{\delta}) \left[\hat{\phi} - \frac{1}{J_l} T_l(x, \hat{\delta})\right]\right\}, \; \gamma > 0 \tag{28}$$

where

$$\frac{\partial T_l}{\partial \delta}(x, \hat{\delta}) = -\frac{K_S}{\pi} \left[\chi_1(x, \hat{\delta}) + \chi_2(x, \hat{\delta})\right] \,. \tag{29}$$

Remark 2. By using the STSMO in (16), (18), we ensure that $\hat{\phi}$ will converge to the real perturbation ϕ in finite-time, which is a stronger convergence property than the one required by the adaptive estimator. However, the effect of measurement noise and parameter or model uncertainties (e.g. in friction) may compromise the exact estimation of ϕ. In this case, by using arguments from the stability of interconnected systems, one can show that the deadzone angle estimation error will not converge asymptotically to zero but it will reach a compact set $[\delta - e_\delta, \delta + e_\delta]$, where $0 < e_\delta \leq c|\phi - \hat{\phi}|$, $c > 0$.

Remark 3. It is interesting to note that the selection of the specific $\mu(x, \hat{\delta})$ function results into a gradient-type adaptive law, which is very common in the literature of adaptive techniques. Although for nonlinearly parametrized systems it does not always guarantee parameter convergence as it does for linear-in-the-parameters systems, it is a natural first choice for the adaptive law.

The complete estimator design is summarized in the following algorithm:

Algorithm 1 Backlash angle estimation

Measured: State variables $\omega_m, \theta_m, \omega_l, \theta_l$.
Output: Deadzone angle estimate $\hat{\delta}$.
1: Design a STSMO for the load velocity (Equations (16), (18)).
2: Estimate the backlash torque (Equation (19)).
3: Design the adaptive estimator for the deadzone angle δ (Equations (26)-(29)).

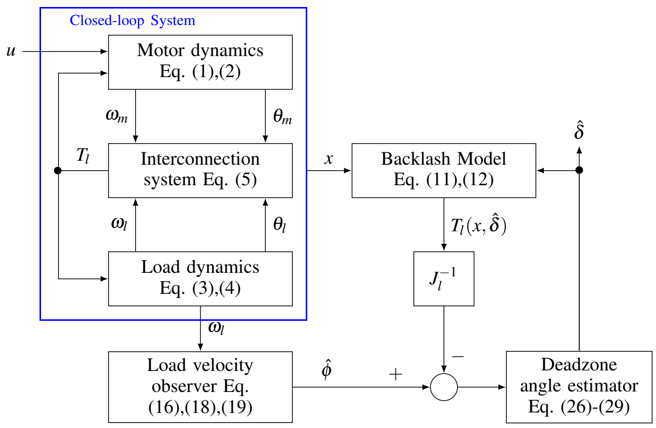

Fig. 4. Block diagram of the closed-loop mechanical drive-train system and the estimation scheme.

4. SIMULATION RESULTS

The drive-train system described in Equations (1)-(5) was simulated in Matlab to assess the performance of the estimation algorithm. The deadzone model in (10) was used to emulate the backlash phenomenon. A Proportional-Integral (PI) controller was used to regulate the drive motor velocity into following a sinusoidal profile $\omega_m^{ref} = \Omega \sin(\nu t)$. A 5% change in the deadzone angle was considered for the evaluation of the algorithm. The velocity measurements were afflicted with white Gaussian noise $w \sim \mathcal{N}(0, \sigma_{meas}^2)$. High precision absolute position encoders were used and the error due to quantization was ignored. Table 2 shows the values of the constants used for the simulations. The compact set $\mathscr{D}$ is the real axis interval $[0, 1]$, the estimator was initialized at $\hat{\delta}(0) = \hat{\delta}_0$, γ was chosen to be 0.1 and the sampling time was 2 ms.

Figure 5 shows the real torque applied in the system according to the deadzone model and its estimation by the STSMO. A small lag can be observed in the estimation of $\hat{\phi}$, which,

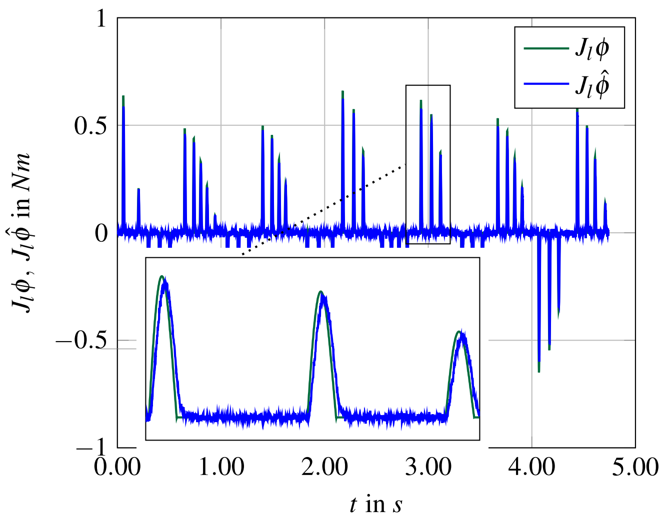

Fig. 5. Real and estimated backlash torque scaled by the load inertia J_l.

however, does not affect the performance of the algorithm. Increasing the gains k_1, k_2 of the observer reduces the delay in estimation but makes the method more sensitive to measurement noise.

The real and estimated deadzone angle, as well as the estimation error, are shown in Figure 6. The plots show that the deadzone angle is estimated with sufficient accuracy in less that 2 s. Specifically, the average steady state estimation error is less than 10^{-3} rad, which the order of magnitude for positioning precision in machine tool applications Gross et al. [2001]. Larger sensor noise has a direct impact on the speed of convergence and the steady-state deviation.

5. CONCLUSIONS

A method for deadzone angle estimation in a single-axis drive-train with backlash has been presented in this paper. The interconnecting torque acting on motor and load was first estimated using a STSMO, followed by an adaptive algorithm that was designed to estimate deadzone angle. The method was tested in a simulation framework, where the adaptive estimator was able to track the real value of the deadzone angle, as well as a 5% increase in the backlash. The parameter convergence was

Table 2. Values used in the simulations

Symbol	Value	Units
J_m, J_l	$8.31 \cdot 10^{-4}$	$\mathrm{kg\,m^2}$
K_S	31.7557	$\mathrm{N\,m\,rad^{-1}}$
D_S	0.0038	$\mathrm{N\,m\,s\,rad^{-1}}$
α	10^5	–
N	1	–
$T_{C,m}, T_{C,l}$	0.0492	$\mathrm{N\,m}$
β_m, β_l	0.0008	$\mathrm{N\,m\,s\,rad^{-1}}$
k_1	32.712	–
k_2	12.0154	–
$\hat{\delta}_0$	0.02	rad
γ	0.1	–
δ_1	0.1	rad
δ_2	0.105	rad
Ω	10	$\mathrm{rad\,s^{-1}}$
ν	$24/(2\pi)$	$\mathrm{rad\,s^{-1}}$
σ_{meas}	0.0316	$\mathrm{rad\,s^{-1}}$

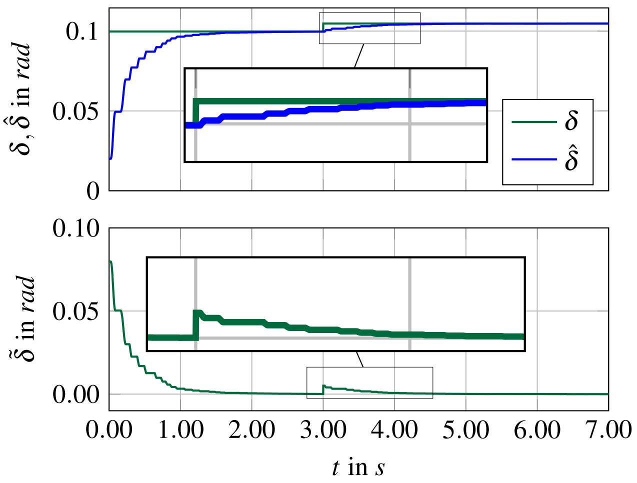

Fig. 6. (Top): Real and estimated change of deadzone angle. (Bottom): Estimation error.

achieved in less than 2 s with precision in the order of 10^{-3} rad. Such precision will allow for use of the estimated parameter in backlash compensation algorithms, that are used in many machine-tool controls. Moreover, detection of changes in the deadzone angle can infer a measure of wear in the mechanical components (i.e. gearing, ball screw, couplings or guides) of the system.

Experimental validation of the method is ongoing.

ACKNOWLEDGEMENTS

The project is sponsored by Siemens AG.

REFERENCES

Davila, J., Fridman, L., and Levant, A. (2005). Second-order sliding-mode observer for mechanical systems. *IEEE Transactions on Automatic Control*, 50(11), 1785–1789.

de Marchi, J.A. (1998). Modeling of dynamic friction, impact backlash and elastic compliance nonlinearities in machine tools, with applications to asymmetric viscous and kinetic friction identification.

Egeland, O. and Gravdahl, J.T. (2002). *Modeling and simulation for automatic control*, volume 76. Marine Cybernetics Trondheim, Norway.

Fridman, L., Moreno, J., and Iriarte, R. (eds.) (2011). *Sliding Modes after the first Decade of the 21st Century: State of the Art (Lecture Notes in Control and Information Sciences)*. Springer, 2012 edition.

Gerdes, J.C. and Kumar, V. (1995). An impact model of mechanical backlash for control system analysis. 5, 3311–3315.

Grip, H.F., Johansen, T.A., Imsland, L., and Kaasa, G.o. (2010). Parameter estimation and compensation in systems with nonlinearly parameterized perturbations. *Automatica*, 46(1), 19–28.

Gross, H., Hamann, J., and Wiegärtner, G. (2001). *Electrical feed drives in automation: basics, computation, dimensioning*. Publicis MCD Corporate Pub.

Hågglund, T. (2007). Automatic on-line estimation of backlash in control loops. *Journal of Process Control*, 17(6), 489–499.

Hovakimyan, N. and Cao, C. (2010). *L1 Adaptive Control Theory: Guaranteed Robustness with Fast Adaptation (Advances in Design and Control)*. Society for Industrial and Applied Mathematics,U.S.

Hovland, G., Hanssen, S., and Gallestey, E. (2002). Nonlinear identification of backlash in robot transmissions. *Proceedings of the 33rd ISR (International Symposium on Robotics) October*, (1), 3–8.

Lagerberg, A. and Egardt, B.S. (2003). Estimation of backlash with application to automotive powertrains. In *Decision and Control, 2003. Proceedings. 42nd IEEE Conference on*, volume 5, 4521–4526 Vol.5.

Levant, A. (1993). Sliding order and sliding accuracy in sliding mode control. *International journal of control*, 58(6), 1247–1263.

Merzouki, R., Davila, J.A., Fridman, L., and Cadiou, J.C. (2007). Backlash phenomenon observation and identification in electromechanical system. *Control Engineering Practice*, 15(4), 447–457.

Merzouki, R. and Cadiou, J.C. (2005). Estimation of backlash phenomenon in the electromechanical actuator. *Control Engineering Practice*, 13(8), 973–983.

Nordin, M. and Gutman, P. (2002). Controlling mechanical systems with backlash - a survey. *Automatica*, 38(10), 1633–1649.

Nordin, M., Galic', J., and Gutman, P.O. (1997). New Models for Backlash and Gear Play.

Shtessel, Y., Edwards, C., Fridman, L., and Levant, A. (2014). *Sliding Mode Control and Observation*. Springer New York, New York, NY.

Stein, J.L. and Wang, C.H. (1998). Estimation of Gear Backlash: Theory and Simulation. *Journal of Dynamic Systems, Measurement, and Control*, 120(1), 74.

Templin, P. (2008). Simultaneous estimation of driveline dynamics and backlash size for control design. *Proceedings of the IEEE International Conference on Control Applications*, 13–18.

Vörös, J. (2010). Modeling and identification of systems with backlash. *Automatica*, 46(2), 369–374.

Appendix A. THE PROJECTION OPERATOR

Let Ω_c be a convex subset of the parameter space $\mathscr{D}$ defined as $\Omega_c \triangleq \{\delta \in \mathscr{D} | h(\delta) \leq c\}$, where $c > 0$ and $h : \mathbb{R} \to \mathbb{R}$ is a smooth convex function. The projection operator is defined as following (Hovakimyan and Cao [2010]):

$$\mathrm{Proj}(\hat{\delta}, \tau) = \begin{cases} \tau & , h(\hat{\delta}) < 0 \\ \tau & , h(\hat{\delta}) \geq 0 \ \& \ \nabla h^T \tau \leq 0 \\ \tau - \frac{\nabla h}{|\nabla h|} \left\langle \frac{\nabla h}{|\nabla h|}, \tau \right\rangle h(\hat{\delta}) & , h(\hat{\delta}) \geq 0 \ \& \ \nabla h^T \tau > 0 \end{cases}$$

In this study the convex function h has been chosen according to Hovakimyan and Cao [2010]:

$$h(\hat{\delta}) \triangleq \frac{(\varepsilon_\delta + 1)\hat{\delta}^2 - \delta_{max}^2}{\varepsilon_\delta \delta_{max}^2} . \tag{A.1}$$

In the above definition of h, δ_{max} is a conservative upper bound for the backlash angle δ and ε_δ is a small positive number. The operator $\langle \cdot, \cdot \rangle$ denotes the inner product, which in this case reduces into a product of real numbers.